Available online at www.sciencedirect.com
ScienceDirect
J. of Supercritical Fluids 41 (2007) 10–19
THE JOURNAL OF Supercritical Fluids
www.elsevier.com/locate/supflu

Solubility of diamines in supercritical carbon dioxide Experimental determination and correlation

Kamel Khimeche [a,b], Paolo Alessi [c], Ireneo Kikic [c], Abdallah Dahmani [b,*]

[a] *Ecole Militaire Polytechnique (EMP), BP 17 Bordj-el-Bahri, Alger, Algeria*
[b] *Laboratoire de Thermodynamique et de Modélisation Moléculaire, Faculté de Chimie, USTHB, BP.32 El-Alia, 16111 Bab-Ezzouar, Alger, Algeria*
[c] *Department of Chemical, Environmental and Raw Materials Engineering, University of Trieste, Piazzale Europa 1, 34127 Trieste, Italy*

Received 9 May 2006; received in revised form 4 September 2006; accepted 8 September 2006

Abstract

In this work, the dynamic method is used for solubility measurements in supercritical carbon dioxide (Sc-CO_2) of some aromatic diamines (1,5-naphthalediamine, and 4,4′-diaminodiphenylmethane) and alkanediamines (1,10-decanediamine and 1,12-dodecanediamine), at pressures from 110 to 200 bar and temperatures from 313.15 to 333.15 K. Solubility in Sc-CO_2 cannot be reported for alkanediamines, since they interact with CO_2. The experimental data for aromatic diamines were well correlated by Peng–Robinson equation of state (PR-EOS), and density-based models (Chrastil and Mendez-Santiago–Teja models). The partial molar volumes of the aromatic diamines in the supercritical fluid (SCF) phase were also estimated, according to the theory developed by Kumar and Johnston.

Keywords: Aromatics diamines; Alkanediamines; Solubility; Supercritical carbon dioxide; Peng–Robinson equation of state; Density-based correlations

1. Introduction

SCF technology has a great application potential in many processes, such as in food, pharmaceutical, biochemical industries and polymer processing [1–8] and is a rapidly developing field of environment-friendly chemistry. As a reaction medium, the attractive physical and toxicological inertness properties of supercritical carbon dioxide have made it superior to conventional organic solvents. Moreover, CO_2 has low critical temperature, good safety properties and it is inexpensive.

Diamines are an important class of compounds applied in different fields of industry and particularly in the synthesis of a number of polymers [2,9–13]. Therefore, knowledge of the solubility of these compounds in Sc-CO_2 and of its dependence on pressure and temperature will be of great importance in process design, particularly in the polymer synthesis in supercritical conditions, where the Sc-CO_2 can act not only as a reaction medium, but also as a catalyst for the reactions in presence of water admixtures [2].

In the present paper, solubility measurements for 1,5-naphthalenediamine (1,5-NDA), 4,4′-diaminodiphenylmethane (DADPM), 1,10-decanediamine (1,10-DDA) and 1,12-dodecanediamine (1,12-DDDA) have been done, using a dynamic method in the pressure range 110–200 bar and the temperature range 313.1–333.1 K. The results were correlated with the Peng–Robinson equation of state (PR-EOS) and the density-based models (Chrastil and Mendez-Santiago–Teja models). The solubility data were also employed for the estimation of partial molar volumes of the aromatic diamines in the supercritical CO_2, according to the theory developed by Kumar and Johnston [14].

2. Experimental

2.1. Materials

The supercritical solvent in this work was carbon dioxide (SIAD, 99.98% purity). Most of the solutes used, 1,5-naphthalenediamine (purity >99%), 1,10-decanediamine (purity >97%) and naphthalene (purity >99%) were supplied from Aldrich. The solutes 4,4′-diaminodiphenylmethane (purity >98%) and 1,12-dodecanediamine (purity >98%) were purchased from Fluka. The alkanediamines are highly hygroscopic

* Corresponding author. Tel.: +213 62 12 99 93; fax: +213 21 24 82 02.
E-mail address: abdahmani@yahoo.fr (A. Dahmani).

0896-8446/$ – see front matter © 2006 Elsevier B.V. All rights reserved.
doi:10.1016/j.supflu.2006.09.004

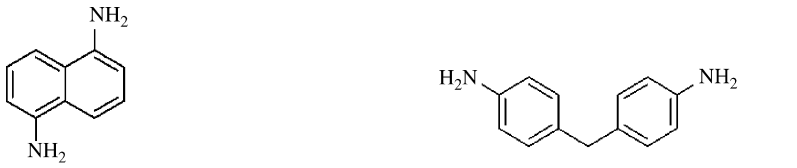

1,5-naphthalenediamine (1,5-NDA) 4,4'-diaminodiphenylmethane (DADPM)

Fig. 1. Chemical structures of the aromatic diamines considered in solubility measurements.

[15], and special care was taken to prepare fully anhydrous samples. The structures of the aromatic diamines are shown in Fig. 1.

Glass beads (30/60 mesh) were used to distribute the solute in the equilibrium cell used for solubility measurements. Ethanol supplied by Sigma (>99% purity) was used as solvent for sample analysis.

2.2. Apparatus and procedures

The thermodynamic properties normal melting temperature T_f and heat of fusion ΔH_{fus} of the different solutes were determined by differential scanning calorimetry (DSC 92 Setaram).

The solubilities of the solids in pure CO_2 were measured using dynamic method. The continuous flow apparatus (Fig. 2) used was calibrated by measuring the solubility of naphthalene in supercritical CO_2 and by comparing the experimental results with literature data. Liquid carbon dioxide was fed through a 2 μm filter to an ISCO 260D high-pressure syringe pump. The CO_2 was compressed and pumped into a preheating coil contained in a temperature-controlled water bath. The fluid passed into an equilibrium cell, which was packed with solute and plugged at each end with glass wool to eliminate entrainment. The fluid was then flashed to atmospheric pressure through a regulating valve, resulting in the precipitation of solute within both the valve and a 0.5 μm filter attached immediately downstream of the valve. Flow rates of CO_2 ranging from 20 to 100 $cm^3\,min^{-1}$ were used. The determination of the solubility was based on the mass of the solute trapped in the valve V_2 and filter F_2 and on the corresponding volume of CO_2. The depressurized CO_2 was quantified with a totalizer flow-meter. Filter and regulating valve were rinsed repeatedly with ethanol in order to collect the solute quantitatively and to prepare the sample for analysis.

Analysis of the solutes was carried by using UV–vis spectrometer (Helios Alpha No. UVA 064422, with spectral game 190-1100). The absorbance was measured (accurate to ±0.001) at wavelengths where the solutes have the absorption maximum.

Quantification was made at wavelengths of 240 nm for 1,5-naphthalenediamine, 245 nm for 4,4′-diaminodiphenylmethane, 205 nm for the alkanediamines (1,10-decanediamine and 1,12-dodecanediamine) and 270 nm for naphthalene. The procedure was repeated until five samples at identical operating conditions show good agreement and the average value was used to calculate the solubility.

During each experiment, the system pressure was measured using a Druck pressure transducer (DPI 260) accurate to ±0.1%. The system temperature was controlled to within ±0.1 K using an immersion circulator (Haake N3) and measured using a RTD platinum probe accurate to ±0.1 K. The gas volume was measured with a precision of 0.01 l and the mass of solute was determined within ±0.2 mg, using a Mettler H31 balance.

Solubility measurements were only started after there was no longer any evidence of impurities in the extract. The measurements were based on the extractions, which yielded homogeneous and uniformly coloured solids.

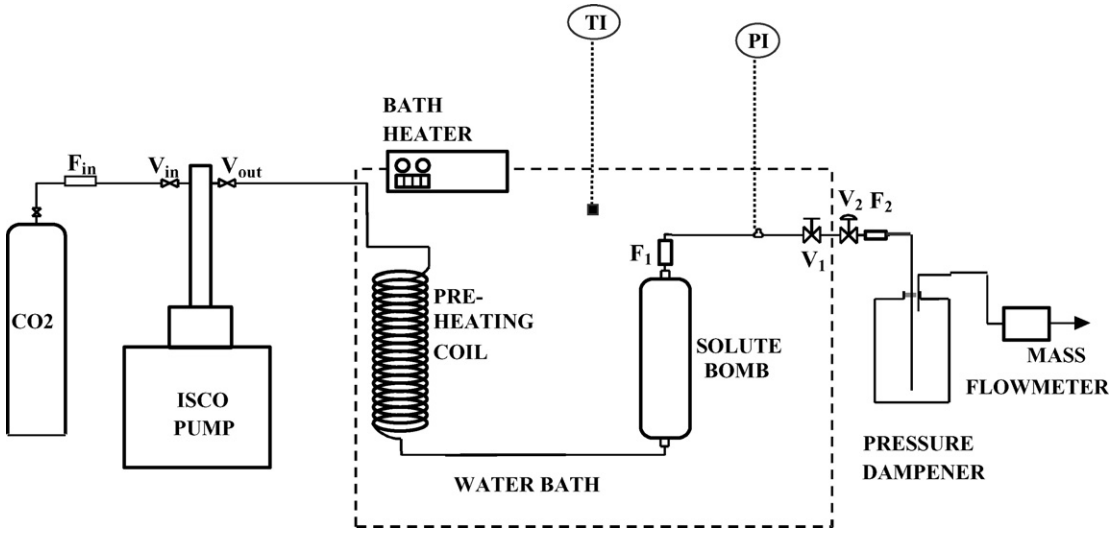

Fig. 2. Experimental apparatus used for the determination of solubility in supercritical CO_2.

Table 1
Experimental solubility data y of naphthalene in supercritical CO_2 and comparison with literature data

T (K)	P (bar)	$y \times 10^3$ (this work)	$y \times 10^3$ (literature)	R.S.D. (%)
308.15	125.0	13.57	14.40[a]	6.12
	146.0	16.58	15.40[a]	7.11
	189.0	17.32	16.90[a]	11.08
	196.9	17.78	17.09[b]	3.88
323.15	100.0	4.83	4.32[c]	10.56
	140.5	22.60	19.80[d]	12.39
328.15	120.1	12.64	12.29[b]	2.77
			9.30[d]	26.42
	130.0	16.17	17.30[d]	6.99
	158.5	34.53	37.93[b]	9.85
333.15	100.0	2.54	2.31[c]	9.05

[a] From Ref. [16].
[b] From Ref. [17].
[c] From Ref. [18].
[d] From Ref. [19].

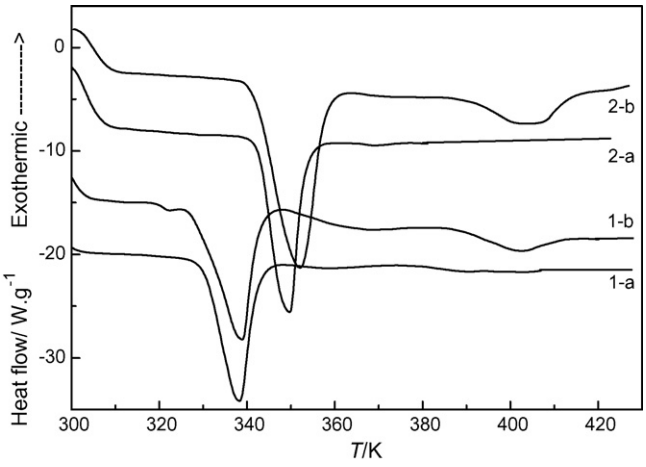

Fig. 3. DSC thermograms for the alkanediamines, obtained with a heating rate 5 K min^{-1} and under nitrogen atmosphere (at 20 ml min^{-1}): 1a and 2a correspond to the pure 1,10-decanediamine and 1,12-dodecanediamine, respectively; 1b and 2b correspond to 1,10-decanediamine and 1,12-dodecanediamine samples, respectively, used in solubility measurements (during 24 h at $P = 180$ bar and $T = 313.15$ K).

3. Results and discussion

3.1. Solubility results

As shown in Table 1, good agreement is observed between the obtained experimental solubility values of naphthalene and literature data. The relative standard deviations (R.S.D.) between the solubility data determined in this work and those reported by different authors [16–19] are globally lower than 13%.

Solubility data are reported only for aromatic diamines. Solubility in Sc-CO_2 cannot be given for alkanediamines (1,10-decanediamine and 1,12-dodecanediamine), since during the experimental determination, they react with carbon dioxide. This reaction is evidenced by the fact that the solute trapped in the valve and the filter is colour different from the starting material. As shown in Fig. 3, a change of thermal behaviour is evidenced by differential scanning calorimetry (DSC) for 1,10-decanediamine and 1,12-decanediamine, which were used previously in solubility measurements at $P = 180$ bar, $T = 313.15$ K and during 24 h.

The first endothermic peaks, which appear at the temperatures 330.08 and 341.90 K, are assigned to the melting of 1,10-decanediamine and 1,12-dodecanediamine, respectively. The second endothermic peaks appearing for each compound in the same temperature range from 393.20 to 415.60 K can be attributed to the melting of the corresponding carbamates.

According to the literature cited, the chemistry between CO_2 and amines [20–22] or CO_2 and diamines [23], is essentially an acid–base equilibrium. Since CO_2 in the presence of water admixtures is acting as a weak acid, we suppose that Sc-CO_2–alkanediamines interactions may be caused principally by water, which still remain in the samples or in carbon dioxide. This in spite the special care taken during experimentation, in order to avoid the hydration problem.

The change of thermal behaviour evidenced by DSC for the alkanediamines, was not observed for aromatic diamines, most probably because of their low reactivity towards carbon dioxide, due principally to their low nucleophilicity.

The attempts done in this work to explain the CO_2–alkanediamines interactions are based on DSC technique. However, these results necessitate a confirmation by other methods such as infrared and NMR spectroscopy analysis.

The average experimental solubility values for 1,5-naphthalenediamine and 4,4′-diaminodiphenylmethane under different conditions of pressure, P, and temperature, T, are summarised in Table 2. The CO_2 density at the given pressure and temperature, were obtained from the IUPAC international thermodynamic tables [24]. The maximum deviation between the measurements was ±4% and gives a good indication of the expected accuracy.

From the data obtained, it is readily observed that the solubility of DADPM and 1,5-NDA increases with increasing pressure at constant temperature, following expected trends. Higher values of solubility are obtained for DADPM + Sc-CO_2 system. These results are expected because of the lower melting temperature of DADPM.

The solubilities for each system as a function of density ρ of the solvent are given in Figs. 4 and 5. Supercritical solubility is strongly influenced by the system temperature and the density of the solvent. The solubility increases with temperature at constant density, due principally to the corresponding increase in vapour pressure.

3.2. Correlation of solubility data

3.2.1. EOS-based models

3.2.1.1. Equation of state. Modelling the solubility of substances in SCF_S is important for SCF-process design.

The solubility data for DADPM and 1,5-NDA were estimated using the classical expression (Eq. (1)) that considers a solid phase, formed by the pure solute (2), in equilibrium with a fluid

Table 2
Experimental mole fraction solubility y_2 for the diamines in supercritical CO_2

T (K)	P (bar)	ρ_{CO_2} (kg m^{-3})	$y_2 \times 10^5$	
			DADPM	1,5-NDA
313.15	110	684.38	3.98	0.51
	120	718.42	6.22	0.73
	130	743.64	7.97	0.87
	140	763.87	9.07	0.94
	150	780.87	9.89	1.02
	160	795.58	10.67	1.11
	170	808.59	11.62	1.18
	190	830.90	12.33	1.28
	200	840.66	12.78	1.30
323.15	110	504.42	2.05	0.26
	120	585.79	3.88	0.59
	130	636.81	6.23	0.77
	140	672.72	7.98	0.92
	150	700.26	9.68	1.06
	160	722.60	11.07	1.15
	170	741.41	12.42	1.25
	190	772.07	13.99	1.39
	200	784.96	14.65	1.43
333.15	110	357.88	0.94	0.19
	120	435.46	2.74	0.42
	130	506.70	5.66	0.62
	140	562.24	7.78	0.87
	150	604.55	9.40	1.09
	160	637.80	12.07	1.25
	170	664.87	13.63	1.39
	190	707.04	15.46	1.57
	200	724.09	16.07	1.62

phase formed by a mixture of solvent (1) and solute (2) [25,26]:

$$y_2 = \frac{P_2^{\text{sub}} \exp[(P - P_2^{\text{sub}})v_2^{\text{s}}/RT]}{P\phi_2^{\text{scf}}} \quad (1)$$

where v_2^{s} and P_2^{sub} are, respectively, the molar volume and sublimation pressure of the solid component (2). The fugacity

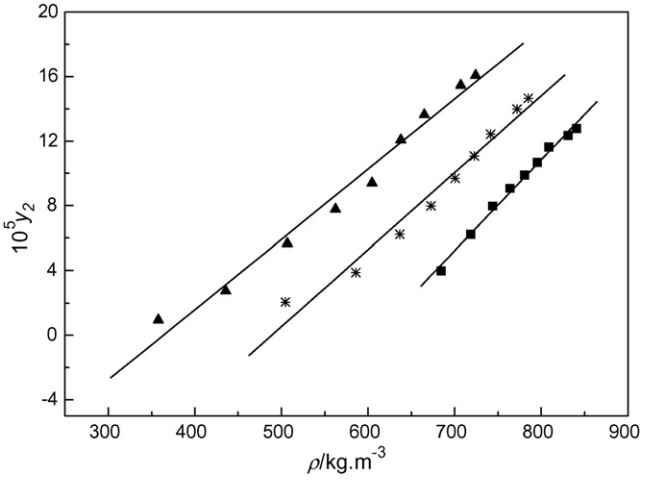

Fig. 4. Mole fraction solubility y_2 of 4,4′-diaminodiphenylmethane in Sc-CO_2 as a function of the density ρ of pure CO_2: (■) 313.15 K; (*) 323.15 K; (▲) 333.15 K; (—) regression fits of the data.

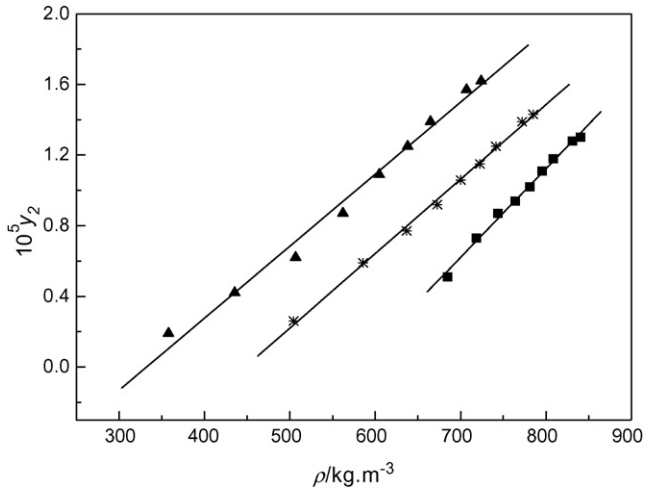

Fig. 5. Mole fraction solubility y_2 of 1,5-naphthalenediamine in Sc-CO_2 as a function of the density ρ of pure CO_2: (■) 313.15 K; (*) 323.15 K; (▲) 333.15 K; (—) regression fits of the data.

coefficient ϕ_2^{scf} is calculated by means of the Peng–Robinson EOS [27,28] expressed by (Eqs. (2)–(7)). The sublimation pressure P_2^{sub} is estimated using the fusion properties of the solid component and the saturation curve derived from this EOS:

$$P = \frac{RT}{v - b} - \frac{a(T)}{v(v + b) + b(v - b)} \quad (2)$$

where P is the pressure; T the temperature; R the gas constant; a and b are the van der Waals energy and volume parameters, respectively. For mixtures, the simple van der Waals mixing rules were used:

$$a = \sum_i^N \sum_j^N x_i x_j a_{ij}, \qquad b = \sum_i^N \sum_j^N x_i x_j b_{ij} \quad (3)$$

$$a_{ij} = \sqrt{a_i a_j}(1 - k_{ij}), \qquad b_{ij} = \frac{b_i + b_j}{2}(1 - l_{ij}) \quad (4)$$

where x is the molar fraction and k_{ij} and l_{ij} are the binary interaction parameters.

Parameters a_i and b_i are given by

$$a_i(T) = 0.457235 \frac{\alpha_i(T_{\text{ri}}, \omega_i) R^2 T_{\text{ci}}^2}{P_{\text{ci}}} \quad (5)$$

with

$$\alpha_i(T_{\text{ri}}, \omega_i) = [1 + (0.37464 + 1.54226\omega_i - 0.26992\omega_i^2) \times (1 - \sqrt{T_{\text{ri}}})]^2 \quad (6)$$

$$b_i = 0.077796 \frac{RT_{\text{ci}}}{P_{\text{ci}}} \quad (7)$$

where ω is the acentric factor; T_{c} and P_{c} the critical constants; T_{r} is the reduced temperature.

For the binary solid–fluid systems, interaction parameters have been calculated from the fitting of solubility data with the

following objective function:

$$\mathrm{OF} = \sum_{i}^{n} \left| \frac{y_i^{\mathrm{CALC}} - y_i^{\mathrm{EXP}}}{y_i^{\mathrm{EXP}}} \right| \quad (8)$$

The Levenberg–Marquardt algorithm is used to find a set of parameters, which minimizes the objective function OF.

The goodness of the calculations is evaluated by the absolute average relative deviation defined as follows:

$$\mathrm{AARD}\ (\%) = \sum_{i}^{n} \left(\left| \frac{y_i^{\mathrm{CALC}} - y_i^{\mathrm{EXP}}}{y_i^{\mathrm{EXP}}} \right| \frac{1}{n} \right) \times 100 \quad (9)$$

where n is the number of solubility data used for obtaining the parameters.

3.2.1.2. Estimation of the sublimation pressure. The sublimation pressure P^{sub} of the solid was estimated, as described in literature, by using the Clapeyron equation [29,30]:

$$\ln \frac{P^{\mathrm{sub}}}{P_{\mathrm{t}}} = -\frac{\Delta H^{\mathrm{sub}}(T)}{R} \left(\frac{1}{T} - \frac{1}{T_{\mathrm{t}}} \right) \quad (10)$$

where T_{t} and P_{t} are the reference conditions chosen at the triple point of the pure component and ΔH^{sub} is the sublimation enthalpy at this temperature, which can be expressed with respect to the fusion and vaporisation enthalpies as

$$\Delta H^{\mathrm{sub}} = \Delta H^{\mathrm{fus}} + \Delta H^{\mathrm{vap}} \quad (11)$$

Using the approximation that the triple point temperature T_{t} can be estimated by the normal fusion temperature, it is thus possible to use experimental values of the normal fusion enthalpy in Eq. (10) and, from the EOS considered, to estimate the reference pressure P_{t} and the vaporisation enthalpy ΔH^{vap} at this temperature.

Table 3
Experimental and predicted properties of the solutes considered[a]

	Solute	
	DADPM	1,5-NDA
MW	198.27	158.20
ΔH_{fus} (kJ mol^{-1})	10.59[b], 9.23[c]	22.29[b]
T_{f} (K)	362.69[b], 363.70[c]	463.10[b], 458.15–460.15[d]
T_{b} (K)	672.15[e]	628.88[f]
v^{s} (ml mol^{-1})	165.22[g]	113.00[e]
v^{l} (ml mol^{-1})	187.75[e]	122.17[g]
T_{c} (K)	925.64[f]	886.30[f]
P_{c} (bar)	34.80[f]	43.39[f]
ω	0.7614[f]	0.7141[f]

[a] Molecular weight MW; enthalpy of fusion ΔH_{fus}; melting temperature T_{f}; boiling temperature T_{b}; molar volume of the solid v^{s}; molar volume of the liquid v^{l}; critical temperature T_{c}; critical pressure P_{c}; acentric parameter ω.
[b] Experimental values of this work.
[c] National Institute of standards and Technology (NIST) data base(http://www.webbook.nist.gov).
[d] Sigma data (http://www.sigma-aldrich.com).
[e] International Chemical Safety Cards (ICSC) data base (http://www.inchem.org/pages/icsc.html).
[f] Estimated by Joback method implemented in PE [32].
[g] Estimated by group contribution methods [31].

Table 4
Results of the solubility data correlation through the PR-EOS[a]

Solute	n	T (K)	Parameters of PR-EOS		
			k_{ij}	l_{ij}	AARD (%)
DADPM	9	313.15	−0.0193	−0.3930	3.06
	9	323.15	−0.1076	−0.6366	2.82
	9	333.15	−0.2166	−0.9434	5.66
1,5-NDA	9	313.15	0.1686	−0.1718	2.61
	9	323.15	0.1525	−0.2430	6.20
	9	333.15	0.1233	−0.3520	6.29

[a] Number of data points used in the correlation (n); binary interactions parameters (k_{ij} and l_{ij}); average absolute relative deviations (AARD).

Parameters such as critical temperature T_{c}, critical pressure P_{c} and the acentric factor ω, which are used to fit the experimental data, must be evaluated. For DADPM and 1,5-NDA, most of these properties were estimated with several group contribution methods, presented in Table 3. A globally good agreement is obtained between the experimental thermal properties used for the modeling and the available literature data.

The measured solubility data for DADPM and 1,5-NDA at 313.15, 323.15 and 333.15 K agree well with the data given by the PR-EOS in the pressure range of 110–200 bar. The Peng–Robinson equation of state with the optimal fitted binary parameters k_{ij} and l_{ij} given in Table 4 at each temperature, resulted in values of AARD lower than 7%. The goodness of the correlation can be seen in Figs. 6 and 7, where the experimental and calculated solubilities for the two aromatic diamines are reported. The negative and lower interaction parameters k_{ij} between CO_2 and DADPM indicate the stronger interactions in this case.

The crossover pressure corresponding to the intersection of the different isotherms was evidenced for each system investigated. The crossover pressures for DADPM and 1,5-NDA, which are, respectively, around 152 and 145 bar, are close to the corresponding calculated values 148 and 151 bar. The crossover point is a consequence of competition of two temperature-dependent

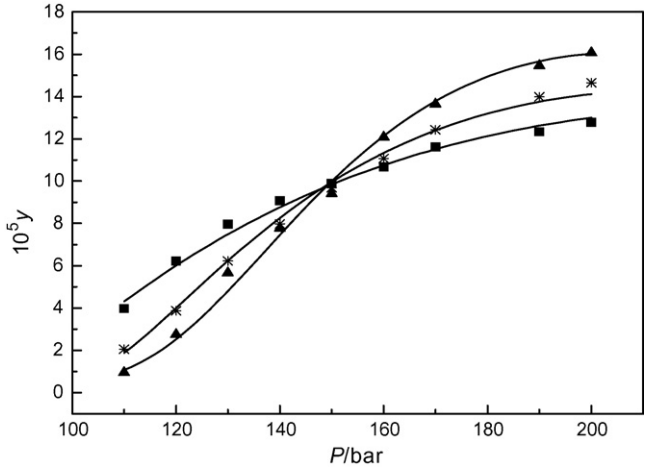

Fig. 6. Mole fraction solubility y_2 of 4,4′-diaminodiphenylmethane in SC-CO_2 measured in this study and correlated by using the PR-EOS: (■) 313.15 K; (*) 323.15 K; (▲) 333.15 K; (—) calculated (PR-EOS model).

Table 5
Results of the solubility data correlation by using Eqs. (12) and (13)[a]

Solute	n	Parameters of Eqs. (12) and (13)						
		A_k	B_k	A_l	B_l	σ_k^2	σ_l^2	AARD (%)
DADPM	27	−0.00986	3.07337	−0.02752	8.23542	0.99634	0.99562	4.68
1,5-NDA	27	−0.00226	0.88007	−0.00901	2.65598	0.97288	0.98554	5.47

[a] Number of data points used in the correlation (n), parameters of Eqs. (12) and (13), respective regression coefficients σ_k^2 and σ_l^2 and average absolute relative deviations (AARD),

Table 6
Results of the solubility data correlation by using the Chrastil model[a]

Solute	n	Parameters of Chrastil model					
		k	α	β	σ^2	AARD (%)	ΔH (kJ mol^{-1})
DADPM	27	5.1667	−5603.10	−17.6756	0.9787	7.7657	46.584
1,5-NDA	27	4.2500	−4620.59	−17.1639	0.9783	1.8167	38.415

[a] Number of data points used in the correlation (n), parameters of Chrastil model (k, α and β), average absolute relative deviations (AARD), regression coefficients σ^2 and ΔH (sum of the heat of vaporisation and heat of solvation of the solute).

factors: vapour pressure of the solute and SCF solvent density. At pressures lower than the crossover pressure, the density effect is dominant, leading to the decrease of the solubility of the solute as function of temperature. For higher pressure than the crossover pressure, the density of the solvent becomes less sensitive to the pressure. This last behaviour leads to the increase of solubility as temperature increases.

The interaction parameters k_{ij} and l_{ij} given in Table 3 were correlated with temperature according to Eqs. (12) and (13):

$$k_{ij} = A_k T + B_k \tag{12}$$

$$l_{ij} = A_l T + B_l \tag{13}$$

where A_k, A_l, B_k and B_l are empirical constants determined by linear regression fitting. The results of data correlation to these equations are reported in Table 5 together with the AARD between experimental and calculated solubility. The goodness of the linear correlation is indicated by the regression coefficients σ_k^2 and σ_l^2 corresponding, respectively, to Eqs. (12) and (13). As it can be seen, these linear relations are able to successfully correlate the interaction parameters for the prediction of solid aromatic diamines + Sc-CO_2 solubility data, in the investigated temperature range.

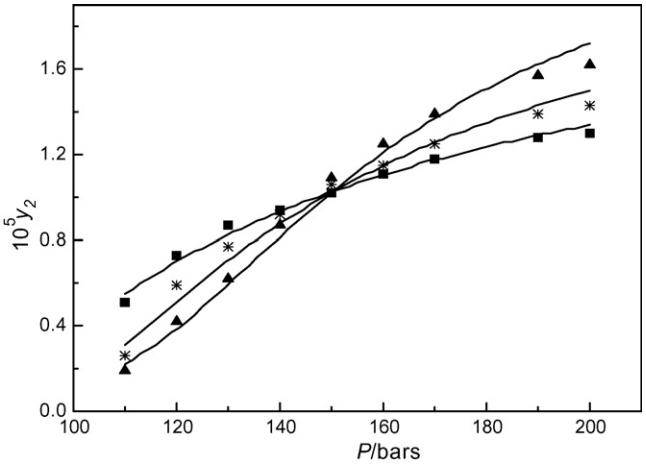

Fig. 7. Mole fraction solubility y_2 of 1,5-naphthalenediamine in SC-CO_2 measured in this study and correlated by using the PR-EOS: (■) 313.15 K; (*) 323.15 K; (▲) 333.15 K; (—) calculated (PR-EOS model).

3.2.2. Density-based correlations of solubility data

In order to correlate the solubility data, two density-based correlations proposed by Chrastil [33] and Mendez-Santiago and Teja [34] were investigated for the DADPM + CO_2 and 1,5-NDA + CO_2 systems. The literature has already provided many examples in which these models were investigated [35–39].

The model proposed by Chrastil relates the solubility of the solute to the density of the supercritical solvent on the assumption that one molecule of a solute, A, associates with k molecules of solvent, B, to form a solute-complex AB_k, in equilibrium with the system.

This model leads to the following equation for the solid solubility:

$$\ln S = k \ln \rho + \frac{\alpha}{T} + \beta \tag{14}$$

where the solubility, S, is calculated by means of Eq. (15):

$$S = \frac{\rho \, \mathrm{MW}_{\mathrm{solute}} \, y_2}{\mathrm{MW}_{\mathrm{SCF}}(1 - y_2)} \tag{15}$$

In Eqs. (14) and (15), ρ (kg m^{-3}) is the density of the pure supercritical fluid; S (kg m^{-3}) the solubility of the solid in the supercritical phase; T the temperature in K; MW the molecular weight; k, α and β are the adjustable parameters of the model. The constant k is the association number, α a constant, defined as $-\Delta H/R$ (where ΔH is the sum of the enthalpies of vaporization and solvation of the solute and R the gas constant) and β depends on the molecular weights of the solute and solvent. The Chrastil model suggests that plots of $\ln S$ for several temperatures are straight lines whose slopes are identical and equal to k. The

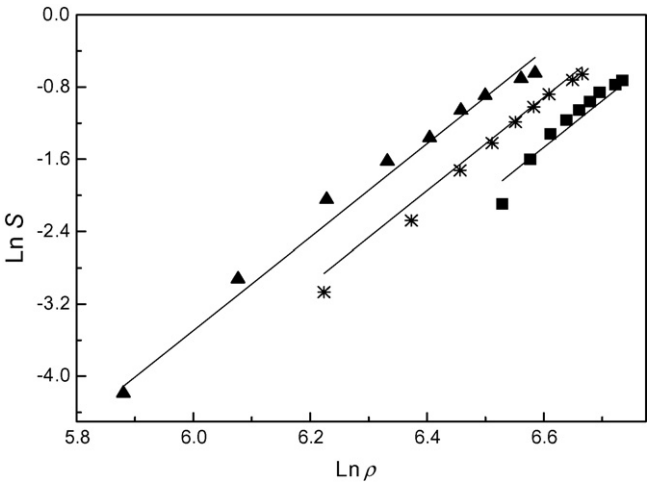

Fig. 8. Logarithmic relationship between the solubility S (kg m^{-3}) of 4,4-diaminodiphenylmethane in Sc-CO_2 and the density ρ (kg m^{-3}) of pure CO_2. Experimental results: (■) 313.15 K; (*) 323.15 K; (▲) 333.15 K; (—) calculated by Eq. (14), Chrastil's model.

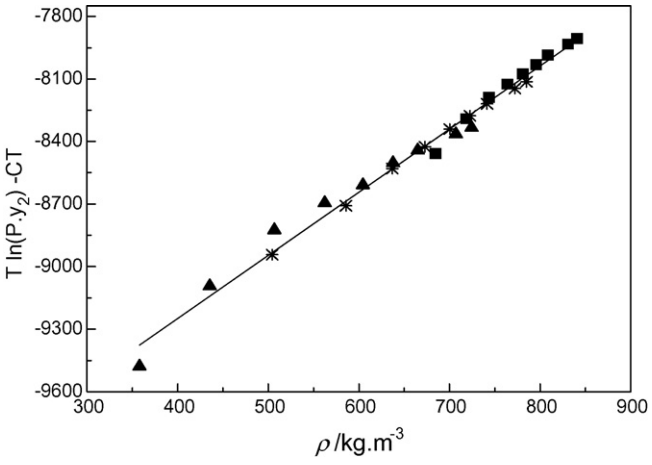

Fig. 10. Solubility of DADPM in pure supercritical CO_2 correlated by using Mendez-Santiago and Teja's model. Experimental results: (■) 313.15 K; (*) 323.15 K; (▲) 333.15 K; (—) calculated by Eq. (16), Mendez-Santiago and Teja's model.

parameters, k, α and β are obtained performing a multiple linear regression on the experimental solubility data.

The values of calculated constants for the binary systems DADPM + Sc-CO_2 and 1,5-NDA + Sc-CO_2 are presented in Table 6. The quality of the correlation is expressed in terms of σ^2 and the average absolute relative deviations (AARD) between experimental and calculated solubility S.

The consistency of the model with measured data can be seen from Figs. 8 and 9 and the values of AARD at different temperatures, which are less than 8%. The results show that the parameters corresponding to the two systems have the same magnitude of values, with higher association number k for the system DADPM + Sc-CO_2. For the DADPM + Sc-CO_2 system, the higher value of the association constant k agrees well with the higher solubility in the supercritical CO_2 observed in this case. However, the highest value of ΔH (sum of heat of solvation and vaporisation of the solute) is in disagreement with the solubility results obtained for this system. So the ΔH values correlated from the solubility data could not be used to explain the possible relation between solubility and the chemical structure of the solutes.

The model proposed by Mendez-Santiago and Teja is based on the simple theory of dilute solutions. According to this model, all the solubility data at different temperatures will coincide to a single straight line once plotted according to equation:

$$T \ln(y_2 P) = A + B\rho + CT \tag{16}$$

where y_2 is the solubility (mole fraction) of the solute in the SCF; T and P the operating temperature and pressure; ρ the density of the SCF; A, B and C are constants considered as independent and obtained by a multiple linear regression of the experimental solubility data.

The correlated results of solubilities of our compounds with the Mendez-Santiago and Teja model are tabulated in Table 7.

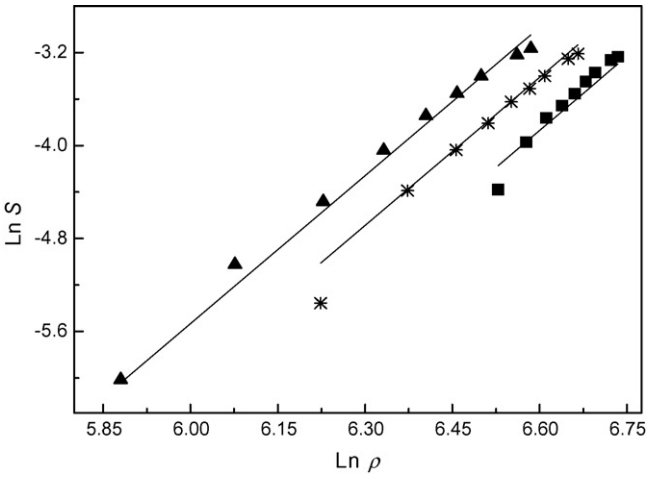

Fig. 9. Logarithmic relationship between the solubility S (kg m^{-3}) of 1,5-naphthalenediamine in Sc-CO_2 and the density ρ (kg m^{-3}) of pure CO_2. Experimental results: (■) 313.15 K; (*) 323.15 K; (▲) 333.15 K; (—) calculated by Eq. (14), Chrastil's model.

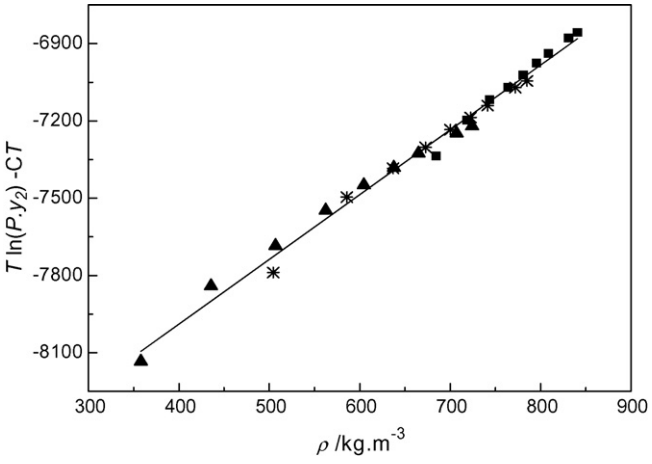

Fig. 11. Solubility of 1,5-NDA in pure supercritical CO_2 correlated by using Mendez-Santiago and Teja's model. Experimental results: (■) 313.15 K; (*) 323.15 K; (▲) 333.15 K; (—) calculated by Eq. (16), Mendez-Santiago and Teja's model.

Table 7
Results of the solubility data correlation by using the Mendez-Santiago and Teja model[a]

Solute	n	Parameters of Mendez-Santiago and Teja model				
		A	B	C	σ^2	AARD (%)
DADPM	27	−10461.30	3.0300	21.5781	0.9792	1.9448
1,5-NDA	27	−8995.170	2.5152	15.9426	0.9843	1.0657

[a] Number of data points used in the correlation (n), parameters of Mendez-Santiago and Teja model (A, B and C), average absolute relative deviations (AARD), and regression coefficients σ^2.

This density-based correlation performs very well for the two aromatic diamine systems with an AARD lower than 2%.

As shown in Figs. 10 and 11, the experimental results were satisfactorily regressed as linear function, with regression coefficients higher than 0.97.

3.3. Estimation of the partial molar volumes of the solutes

According to Kumar and Johnston [14], the dependence of the solubility y_1 of the solute with its partial molar volume in the vicinity of the critical density of the SCF, can be expressed by the following equation:

$$\ln y_2 = -C_2 + \ln\left(\frac{P_2^{\mathrm{vp}}}{\rho_{\mathrm{c}} RT}\right) + \frac{PV_2^{\mathrm{S}}}{RT} - \left(\frac{\bar{V}_2}{RT\kappa_T}\right)_{\rho_{\mathrm{r}}=1} \ln \rho_{\mathrm{r}} \quad (17)$$

where y_2 represents the equilibrium mole fraction of the solute in the SCF; P_2^{S} and V_2^{S} the vapor pressure and molar volume of the solid solute; R the universal gas constant; $\bar{V}_2$ the partial molar volume of the solute in the SCF phase; $\kappa_T = [(1/\rho)(\partial\rho/\partial P)_{T,y_1}]$ and $\rho_{\mathrm{r}} = \rho/\rho_{\mathrm{c}}$ the isothermal compressibility and reduced density of the phase; T is the operating temperature.

The partial molar volumes of the solute in the SCF phase, $\bar{V}_2$, are much larger than the molar volume of the solute, V_2^{s}. The third term in Eq. (17) was considered as constant in the region of interest. Eq. (17) may thus be simplified as

$$\ln y_2 = C_0 - \left(\frac{\bar{V}_2}{RT\kappa_T}\right)_{\rho_{\mathrm{r}}=1} \ln \rho_{\mathrm{r}} \quad (18)$$

Eq. (18) implies that in the approximate density interval $0.5 \le \rho_{\mathrm{r}} \le 2.0$, the log of the mole fraction of the solubility of the solute in a SCF varies linearly with the log of the density of the SCF phase. The slope of this line is the ratio of the partial molar volume of the solute in the SCF phase to the isothermal compressibility of the fluid phase. This ratio is considered as independent of ρ_{r}, thus the knowledge of the value of κ_T and the slope of the $\ln y_2$ versus $\ln \rho_{\mathrm{r}}$ at this temperature permits the estimation of $\bar{V}_2$ under these conditions.

As demonstrated in Figs. 12 and 13, the systems investigated display linearity when plotted as $\ln y_2$ versus $\ln \rho_{\mathrm{r}}$. This linearity is not observed when $\ln y_2$ values were plotted versus ρ_{r}. The slopes of the line $\ln y_1$ versus $\ln \rho_{\mathrm{r}}$ were computed by linear squares fit for the DADPM + Sc-CO_2 and 1,5-NDA + Sc-CO_2 systems at different temperatures. The quality of the linear correlation is expressed in terms of σ^2. Partial molar volumes were then deduced from the determined slopes and the values of κ_T for CO_2 at the appropriate P–T conditions.

The results obtained are recapitulated in Table 8. As it can be seen, the partial molar volume for each solute decreases as temperature increases. Higher absolute values of $\bar{V}_2$ are observed for DADPM. The partial molar vol-

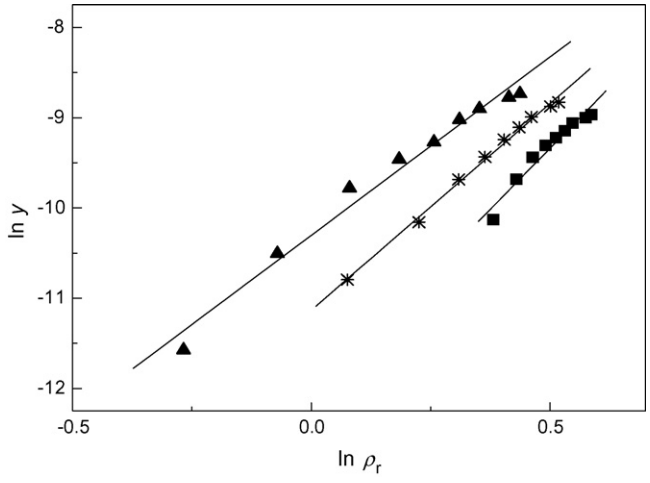

Fig. 12. Plot of $\ln y_2$ vs. $\ln \rho_{\mathrm{r}}$ for the solubility of DADPM in supercritical CO_2: (■) 313.15 K; (*) 323.15 K; (▲) 333.15 K; (—) regression fits of the experimental data.

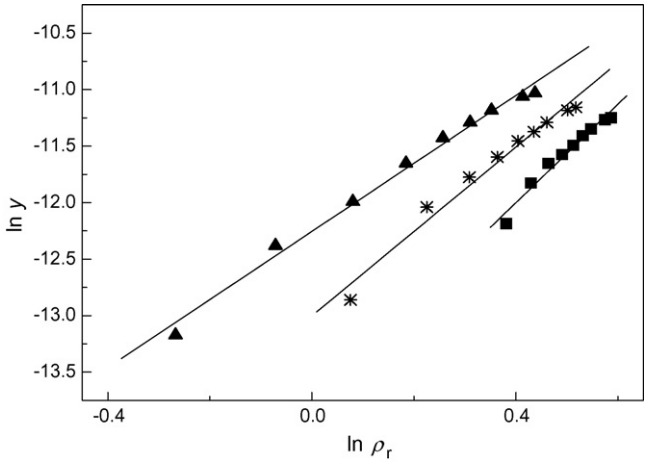

Fig. 13. Plot of $\ln y_2$ vs. $\ln \rho_{\mathrm{r}}$ for the solubility of 1,5-NDA in supercritical CO_2: (■) 313.15 K; (*) 323.15 K; (▲) 333.15 K; (—) regression fits of the experimental data.

Table 8
Slopes computed from Eq. (18) and the corresponding partial molar volumes $\bar{V}_2$ of the solute for DADPM + Sc-CO_2 and 1,5-NDA + Sc-CO_2 systems at different temperatures

System	T (K)	Slope at $\rho_r = 1$	σ^2	$\bar{V}_2$ ($cm^3\ mol^{-1}$)
DADPM/CO_2	313.15	5.41	0.9512	−8078.62
	323.15	4.58	0.9957	−2971.12
	333.15	3.95	0.9792	−1625.97
1,5-NDA/CO_2	313.15	4.36	0.9674	−6510.68
	323.15	3.73	0.9768	−2419.71
	333.15	3.01	0.9905	−1239.03

umes $\bar{V}_2$ of the DADPM and 1,5-NDA in the vicinity of the critical point of the solvent, which are difficult to measure experimentally, are then estimated by following the theory developed by Kumar and Johnston. As reported by these authors, the data calculated for naphthalene + CO_2 and naphthalene + ethylene systems according to this theory were in good agreement with experimental data. However, the results of this work necessitate a confrontation with experimental measurements.

4. Conclusion

The solubilities of 1,5-naphthalenediamine and 4,4′-diaminodiphenylmethane at 313.15, 323.15 and 333.15 K were determined in supercritical carbon dioxide for pressure ranging from 110 to 200 bar. The maximum deviation between the measurements was ±4%.

Solubility data of 4,4′-diaminodiphenylmethane are higher compared with solubility of 1,5-naphthalenediamine at the same conditions. Solubility in supercritical CO_2 was not observed for alkanediamines, which interact with the solvent. The solubility results for the aromatic diamines show trends expected for the solubility of non-volatile organic molecules, with crossover pressures, which are around 152 and 145 bar for the DADPM + Sc-CO_2 and 1,5-NDA + Sc-CO_2 systems, respectively.

Peng–Robinson model is able to reproduce experimental data correctly and with low deviations from the experimental values. The two density-based models investigated (Chrastil and Mendez-Santiago–Teja models) were able to successfully correlate the experimental solid aromatic diamine + Sc-CO_2 solubility data. They have the advantage to predict the solubility in Sc-CO_2, without need to the estimation of the solid properties.

Better agreement with experimental solubility data is obtained with Mendez-Santiago–Teja's model. Values of AARD lower than 2% were observed.

Solubility data were used to estimate the partial molar volume $\bar{V}_2$ for each aromatic diamine in the supercritical phase, according to the theory developed by Kumar and Johnston. Higher absolute values of $\bar{V}_2$, which decrease as temperature increases, were obtained for DADPM in the temperature range investigated.

References

[1] M.P. Srinivasan, Y. Gu, R. Begum, Imidisation of Langmuir–Blodgett films using a supercritical medium, Colloids Surf. A: Physicochem. Eng. Aspects 198–200 (2002) 527–534.
[2] E.E. Said-Galiyev, S.Y. Vygodskii, L.N. Nikitin, R.A. Vinokur, M.O. Gallyamov, I.V. Pototskaya, V.V. Kireev, A.R. Khokhlov, K. Shaumburg, Synthesis of polyimides in supercritical carbon dioxide, J. Supercrit. Fluids 26 (2003) 147–156.
[3] O. Guney, A. Akgerman, Synthesis of controlled-release products in supercritical medium, AIChE J. 48 (2002) 851–866.
[4] B. Subramaniam, R.A. Rajewski, K. Snavely, Pharmaceutical processing with supercritical carbon dioxide, J. Pharm. Sci. 86 (1997) 885–890.
[5] B. Guzel, A. Akgerman, Mordant dyeing of wool by supercritical processing, J. Supercrit. Fluids 18 (2000) 247–252.
[6] S.J. Macnaughton, I. Kikic, N.R. Foster, P. Alessi, A. Cortesi, I. Colombo, Solubility of anti-inflammatory drugs in supercritical carbon dioxide, J. Chem. Eng. Data 41 (1996) 1083–1086.
[7] R. Murga, M.T. Sanz, S. Beltran, J.L. Cabezas, Solubility of some phenolic compounds contained in grape seeds, in supercritical carbon dioxide, J. Supercrit. Fluids 23 (2002) 113–121.
[8] N. Ajzenberg, F. Trabelsi, F. Recasens, Review. What's new in industrial polymerization with supercritical Solvents? A Short Review, Chem. Eng. Technol. 23 (2000) 829–839.
[9] C. Konin, A. Delmotte, P. Larno, B. Van Mele, Influence of polymerization conditions on melt crystallisation of partially aliphatic polyimides, Polymer 39 (1998) 3697–3702.
[10] M. Nagata, Novel regular network polyimide films from mellitic acid and aliphatic and aromatic diamines or diisocyanates, Polymer 36 (1995) 2657–2662.
[11] A. Diaf, E.J. Beckman, Thermally reversible polymeric sorbents for acid gazes. III. CO_2-sorption enhancement in polymer-anchored amines, React. Funct. Polymers 27 (1995) 45–51.
[12] M. Aresta, A. Dibenedetto, E. Quaranta, Reaction of aromatic diamines with diphenylcarbonate catalysed by phosphorous acids: a new clean synthetic route to mono- and dicarbamates, Tetrahedron 54 (1998) 14145–14156.
[13] N.R. Prasad, N. Gupta, Template synthesis of Mn(II) complexes of tetraazamacrocycles derived from diaminoalkanes and 3,4-hexanedione or benzil, J. Serb. Chem. Soc. 68 (2003) 455–461.
[14] S.K. Kumar, K.P. Johnston, Modeling the solubility of solids in supercritical fluids with density as the independent variable, J. Supercrit. Fluids 1 (1988) 15–22.
[15] L. Dall'acqua, G. Della Gatta, B. Nowicka, P. Ferloni, Enthalpies and entropies of fusion of ten alkane-α,ω-diamines H_2N–$(CH_2)_n$–NH_2 where $3 \le n \le 12$, J. Chem. Thermodyn. 34 (2002) 1–12.
[16] V. Pauchon, Z. Cissé, M. Chavret, J. Jose, A new apparatus for the dynamic determination of solid compounds solubility in supercritical carbon dioxide. Solubility determination of triphenylmethane, J. Supercrit. Fluids 32 (2004) 115–121.
[17] M. McHugh, M.E. Paulaitis, Solid solubilities of naphthalene and biphenyl in supercritical carbon dioxide, J. Chem. Eng. Data 25 (1980) 326–329.
[18] Z. Suoqi, W. Renan, Y. Guanghua, A method for measurement of solid solubility in supercritical carbon dioxide, J. Supercrit. Fluids 8 (1995) 15–19.
[19] A. Zúniga-Moreno, L.A. Galicia-Luna, L.E. Camacho-Camacho, Measurements of solid solubilities and volumetric properties of naphthalene + carbon dioxide mixtures with a new assembly taking advantage of a vibrating tube densitometer, Fluid Phase Equilib. 234 (2005) 151–163.
[20] M. Selva, P. Tundo, A. Perosa, The synthesis of alkyl carbamates from primary aliphatic amines and dialkyl carbonates in supercritical carbon dioxide, Tetrahedron Lett. 43 (2002) 1217–1219.
[21] E.M. Hampe, D.M. Rudkevich, Exploring reversible reactions between CO_2 and amines, Tetrahedron 59 (2003) 9619–9625.
[22] M. Aresta, A. Dibenedetto, E. Quaranta, M. Boscolo, R. Larsson, The kinetics and mechanism of the reaction between carbon dioxide and a series of amines. Observation and interpretation of an isokinetic effect, J. Mol. Catal. A: Chem. 174 (2001) 7–13.

[23] T. Yamaguchi, C. Koval, R.D. Noble, C.N. Bowman, Transport mechanism of carbon dioxide through perfluorosulfonate ionomer membranes containing an amine carrier, Chem. Eng. Sci. 51 (1996) 4781–4789.
[24] S. Angus, B. Armstrong, K.M. de Reuck, IUPAC. International Thermodynamic Tables of the Fluid State: Carbon dioxide, vol. 3, Pergamon Press, Oxford, UK, 1976.
[25] S.K. Jha, G. Madras, Modeling the solubilities of high molecular weight *n*-alkanes in supercritical carbon dioxide, Fluid Phase Equilib. 225 (2004) 59–62.
[26] G. Madras, C. Kulkarni, J. Modak, Modeling the solubilities of fatty acids in supercritical carbon dioxide, Fluid Phase Equilib. 209 (2003) 207–213.
[27] J.O. Valderrama, V.H. Alvarez, Temperature independent mixing rules to correlate the solubility of solids in supercritical carbon dioxide, J. Supercrit. Fluids 32 (2004) 37–46.
[28] S. Colussi, N. Elvassore, I. Kikic, A comparison between semi-empirical and molecular based equations of state for describing the thermodynamic of supercritical micronization process, J. Supercrit. Fluids 39 (2006) 118–126.
[29] E. Neau, S. Garnier, L. Avaullée, A consistent estimation of sublimation pressures using a cubic equation of state and fusion properties, Fluid Phase Equilib. 164 (1999) 173–186.
[30] S. Garnier, E. Neau, P. Alessi, A. Cortesi, I. Kikic, Modelling solubility of solids in supercritical fluids using fusion properties, Fluid Phase Equilib. 158–160 (1999) 491–500.
[31] L.H. Nelken, Densities of vapors, liquids and solids, in: W.J. Lyman, F.W. Reehl, D.H. Rosenblatt (Eds.), Handbook of Chemical Property Estimation Methods, American Chemical Society, Washington, DC, 1990 (Chapter 19).
[32] S. Petkov, O. Pfohl, G. Brunner, PE—A Program to Calculate Phase Equilibria, Herbert Utz Verlag, München, 2000.
[33] J. Chrastil, Solubility of solids and liquids in supercritical gases, J. Phys. Chem. 86 (1982) 3016–3021.
[34] J. Mendez-Santiago, A.S. Teja, Solubility of solids in supercritical fluids: consistency of data and a new model for cosolvent systems, Ind. Eng. Chem. Res. 39 (2000) 4767–4771.
[35] P. Coimbra, M.H. Gil, C.M.M. Duarte, B.M. Heron, H.C. de Soussa, Solubility of a spiroindolinonaphthoxazine photochromic dye in supercritical carbon dioxide: experimental determination and correlation, Fluid Phase Equilib. 238 (2005) 120–128.
[36] Z. Huang, X.-W. Yang, G.-B. Sun, S.-W. Song, S. Kawi, The solubilities of xanthone and xanthene in supercritical carbon dioxide. Structure effect, J. Supercrit. Fluids 36 (2005) 91–97.
[37] M. Skerget, Z. Knez, M. Habulin, Solubility of β-carotene and oleic acid in dense CO_2 and data correlation by a density based model, Fluid Phase Equilib. 109 (1995) 131–138.
[38] C.A. Nalesnik, B.N. Hansen, J.T. Hsu, Solubility of pure taxol in supercritical carbon dioxide, Fluid Phase Equilib. 146 (1998) 315–323.
[39] P. Subra, S. Castellani, H. Ksibi, Y. Garrabos, Contribution to the determination of the solubility of β-carotene in supercritical carbon dioxide and nitrous oxide: experimental data and modeling, Fluid Phase Equilib. 131 (1997) 269–289.